Structural Evaluation and Solution Integrity of Alkali Metal Salt Complexes of the Manganese 12-Metallacrown-4 (12-MC-4) Structural Type

Brian R. Gibney,† Hsin Wang, Jeff W. Kampf, and Vincent L. Pecoraro*

Willard H. Dow Laboratories, Department of Chemistry, The University of Michigan, Ann Arbor, Michigan 48109-1055

Received April 4, 1996[⊗]

The preparation of a variety of salt complexes of [12-$MC_{Mn(III)N(shi)}$-4] (**1**) provides the structural basis for the first quantitative investigation of the cation and anion selectivity of metallacrowns. The preparation, X-ray crystal structures, and solution integrities of crystalline salts $(LiCl_2)$[12-$MC_{Mn(III)N(shi)}$-4]$^-$ ([$(LiCl_2)$·**1**]$^-$), (Li(trifluoroacetate))[12-$MC_{Mn(III)N(shi)}$-4] ([(LiTFA)·**1**]), (Li)[12-$MC_{Mn(III)N(shi)}$-4]$^+$ ([(Li)·**1**]$^+$), $(NaBr)_2$[12-$MC_{Mn(III)N(shi)}$-4] ([$(NaBr)_2$·**1**]), and $(KBr)_2$[12-$MC_{Mn(III)N(shi)}$-4] ([$(KBr)_2$·**1**]) of the metallacrown [12-$MC_{Mn(III)N(shi)}$-4] (**1**) are described. Each salt complex of the metallacrown forms from a generic one-step, high-yield synthesis giving 1:1 metal:metallacrown adducts with lithium and 2:1 metal:metallacrown complexes with sodium and potassium ions. On the basis of synthetic preference, the trend for the cation affinity is $Li^+ > Na^+ > K^+$ and that for anion affinity is $Cl^- > Br^- > TFA^- > F^- \approx I_3^-$. The 12-metallacrown-4 structural parameters compare favorably with those of 12-crown-4, an organic crown ether, as well as with those of the topologically similar alkali metal complexes of porphyrin and phthalocyanine dianions, solidifying the structural analogy between metallacrowns and crown ethers. The solution integrities of the alkali metal halide salts of [12-$MC_{Mn(III)N(shi)}$-4] were confirmed by using paramagnetically shifted ^{1}H NMR, FAB-MS, ESI-MS, and UV−vis spectroscopies. Analysis of the ^{1}H NMR spectra and ESI-MS of the complexes proves that both the halide ions and the cations remain bound to the metallacrown upon dissolution. Investigations of metallacrown ligand exchange rates demonstrate that the metallacrowns are inert to ligand exchange in DMF and acetonitrile. This broad series of salt complexes of a single metallacrown allows for comparison of the structural features influencing the stability and specificity of *joint* cation/anion binding in this relatively new molecular class. X-ray parameters: $(LiCl_2)$[12-$MC_{Mn(III)N(shi)}$-4]$^-$ ([$(LiCl_2)$·**1**]$^-$), triclinic space group, $P\bar{1}$, $a = 12.516(2)$ Å, $b = 13.780(2)$ Å, $c = 19.943(3)$ Å, $\alpha = 85.20(1)°$, $\beta = 84.57(1)°$, $\gamma = 72.18(1)°$, $V = 5059(2)$ Å^3, $Z = 2$, $R = 0.0773$, $R_w = 0.0887$; (Li(trifluoroacetate))[12-$MC_{Mn(III)N(shi)}$-4] ([(LiTFA)·**1**]), (monoclinic space group, *Cc*, $a = 20.261(6)$ Å, $b = 19.577(5)$ Å, $c = 16.134(5)$ Å, $\beta = 99.81(2)°$, $Z = 4$, refined on $|F|^2$, $wR^2 = 0.2071$; (Li)[12-$MC_{Mn(III)N(shi)}$-4]$^+$ ([(Li)·**1**]$^+$), (monoclinic space group, $P2_1/n$, $a = 14.814(4)$ Å, $b = 14.909(3)$ Å, $c = 32.26(1)$ Å, $\beta = 102.42(2)°$, $Z = 4$, refined on $|F|^2$, $wR^2 = 0.0684$; $(NaBr)_2$[12-$MC_{Mn(III)N(shi)}$-4] ([$(NaBr)_2$·**1**]), monoclinic space group, $P2_1/n$, $a = 14.131(4)$ Å, $b = 13.845(3)$ Å, $c = 16.539(4)$ Å, $\beta = 96.17(2)°$, $Z = 2$, $R = 0.0416$, $R_w = 0.0419$; $(KBr)_2$[12-$MC_{Mn(III)N(shi)}$-4] ([$(KBr)_2$·**1**]), monoclinic space group, $P2_1/n$, $a = 11.654(3)$ Å, $b = 17.392(5)$ Å, $c = 16.786(5)$ Å, $\beta = 98.40(2)°$, $Z = 2$, $R = 0.0649$, $R_w = 0.0850$.

The crown ethers[1−6] are the classic synthetic ionophores, and the revelation of their cation-binding properties launched the rich field of host−guest chemistry.[7−12] The binding of cations into the formally neutral crown cavities follows the hole-size relationship to a first approximation.[13] Preorganization[14−16] of the crown oxygen donors by synthetic design has yielded crown compounds with increased cation affinities, including a conformationally rigid 18-C-6.[17] Appending of charged donor groups (lariat ethers)[18−20] that bridge the ring methylene carbons to the core metal increases the metal ion affinity as well as reduces the charge on the overall complex. Increasing the denticity of the crowns and construction of three-dimensional cavities (cryptands)[21−25] also increase the binding affinities of the crowns for alkali metals. Aside from topological design

† Current address: Department of Biochemistry and Biophysics, B501 Richards Bldg., University of Pennsylvania, Philadelphia, PA 19104.

⊗ Abstract published in *Advance ACS Abstracts,* September 15, 1996.

(1) Pederson, C. J. *J. Am. Chem. Soc.* **1967**, *89*, 7017.
(2) Pedersen, C. J. *J. Am. Chem. Soc.* **1967**, *89*, 2495.
(3) Pedersen, C. J. *J. Am. Chem. Soc.* **1970**, *92*, 386.
(4) Pedersen, C. J. *J. Am. Chem. Soc.* **1970**, *92*, 391.
(5) Pedersen, C. J.; Frensdorf, H. K. *Angew. Chem., Intl. Ed. Engl.* **1972**, *11*, 1.
(6) Pedersen, C. J. *Angew. Chem., Int. Ed. Engl.* **1988**, *27*, 1021.
(7) Cram, D. J.; Cram, J. M. *Acc. Chem. Res.* **1978**, *11*, 8.
(8) Cram, D. J.; Lein, G. M. *J. Am. Chem. Soc.* **1985**, *107*, 3657.
(9) Cram, D. J. *Angew. Chem., Int. Ed. Engl.* **1988**, *27*, 1009.
(10) Hiraoka, M. *Crown Ethers and Analogous Compounds*; Elsevier: New York, 1992; Vol. 45, p 485.
(11) Weber, E.; Toner, J. L.; Goldberg, I.; Vögtle, F.; Laidler, D. A.; Stoddart, J. F.; Bartsch, R. A.; Liotta, C. L. *Crown Ethers and Analogs*; John Wiley & Sons: New York, 1989; p 558.
(12) Cooper, S. R. *Crown Compounds: Toward Future Applications*; VCH Publishers: New York, 1992; p 325.
(13) Gokel, G. W.; Goli, D. M.; Minganti, C.; Echegoyen, L. *J. Am. Chem. Soc.* **1983**, *105*, 6786−6788.
(14) Cram, D. J.; Kaneda, T.; Helgeson, R. C.; Lein, G. M. *J. Am. Chem. Soc.* **1979**, *101*, 6752.
(15) Cram, D. J.; Lein, G. M.; Kaneda, T.; Helgeson, R. C.; Knobler, C. B.; Maverick, E.; Trueblood, K. N. *J. Am. Chem. Soc.* **1981**, *103*, 6228.
(16) Cram, D. J.; Kaneda, T.; Helgeson, R. C.; Brown, S. B.; Knobler, C. B.; Maverick, E.; Trueblood, K. N. *J. Am. Chem. Soc.* **1985**, *107*, 3645.
(17) Li, G.; Still, W. C. *J. Am. Chem. Soc.* **1993**, *115*, 3804.
(18) Gokel, G. W.; Dishong, D. M.; Diamond, C. J. *J. Chem. Soc., Chem. Commun.* **1980**, 1053.
(19) Gokel, G. W.; Echegoyen, L.; Kim, M. S.; Eyring, E. M.; Petrucci, S. *Biophys. Chem.* **1987**, *26*, 225.
(20) Gokel, G. W. *J. Chem. Soc. Rev.* **1992**, 39.
(21) Lehn, J.-M.; Sauvage, J. P. *J. Am. Chem. Soc.* **1975**, *97*, 6700−6707.
(22) Lehn, J.-M. *Acc. Chem. Res.* **1978**, *11*, 49.
(23) Lehn, J.-M.; Montavon, F. *Helv. Chim. Acta* **1978**, *61*, 67.
(24) Lehn, J.-M. *Science* **1985**, *219*, 1177.

S0020-1669(96)00371-0 CCC: $12.00

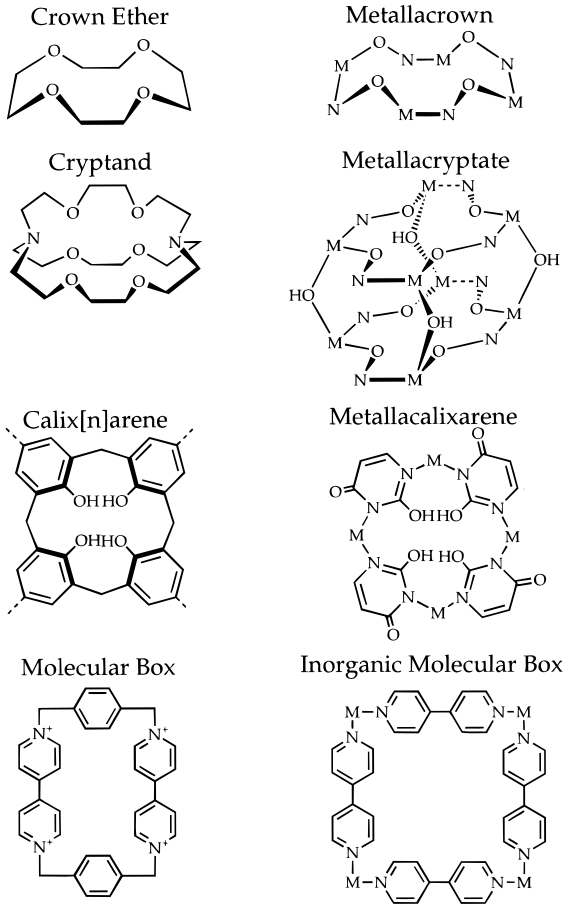

Figure 1. Organic and inorganic molecular recognition structure types.

aspects, the incorporation of nitrogen (azacrown ethers)[26] and sulfur (crown thiaethers) into the heteroatom positions modulates the metal ion selectivity.

Our approach to heteroatom substitution, the metallacrown analogy,[27] is to incorporate transition metal ions and nitrogen atoms into the methylene positions of the crown ethers as illustrated in Figure 1. The metallacrown substitutes an $[M^{x+}\text{-}NO]_x$ linkage for the $[CH_2CH_2O]_x$ repeat unit of the crown ethers while retaining comparable cavity sizes. Stabilization of transition metals in the metallacrown cavities is accomplished by the use of formally charged hydroxamate oxygens in the core as well as lariat ether-like anions bridging between the ring and core metals. Metallacrowns have been characterized in 9-MC-3,[28−30] 12-MC-4,[31−36] 15-MC-5,[37] and metallacryptate[38] structural motifs, incorporating 7 metals in ring positions and 20 metals in the metallacrown cavities. In each case, a multifunctional hydroxamic acid (e.g., salicylhydroxamic acid) or oxime is used to stabilize the metallacrown ring. Incorporation of transition metals into the metallacrowns affords properties not found in the simple organic crowns, such as redox activity, strong absorption spectra, and paramagnetism. The recent preparation of heterometallic metallacrowns leads to site-differentiated structures with further variations in physical properties.[36]

Structurally, the concept of heteroatom substitution at the carbon atom positions of molecular host compounds can be applied to a variety of topological designs as shown in Figure 1. Recently a novel class of metallacrowns containing carbon in the macrocycle, i.e., a $[CuNCO]_6$ core, was reported that binds either Na(I) or Cu(II) in the cavity.[39,40] Additionally, the use of a $[Pt(en)]^{2+}$ moiety in the methylene position of a calix[n]-arene[41,42] has afforded a tetranuclear complex that structurally resembles a calix[4]arene, as shown in Figure 1.[43] We have previously noted the structural similarities between 9-$MC_{(V\text{-}(V)O)N(nha)}$-3 and calix[3]arene.[30] Finally, the use of $[Pd(en)]^{2+}$ and $[Pt(1,3\text{-bis(diphenylphosphino)propane})]^{2+}$ as the corners of inorganic molecular boxes capable of binding neutral organic guests has been reported.[44,45] Thus, these metallacrowns, metallocalix[*n*]arenes, and inorganic molecular boxes represent the initiation of inorganic molecular hosts capable of selectively binding cationic, anionic, and neutral guests.[46]

In this paper, we report the formation of alkali metal halide salt complexes of the metallacrown, [12-$MC_{Mn(III)N(shi)}$-4] (**1**), which is a structural and functional[47] inorganic analogue of 12-C-4. The synthetic procedure is general and leads to high yields and crystals suitable for X-ray analysis. From these data, a direct structural comparison can be made between a wide range of metallacrowns as well as between alkali metal metallacrown, crown ether, porphyrin, and phthalocyanine complexes. Direct evidence for the retention of the general solid state structure in solution is presented. These studies firmly establish the structural analogy between metallacrowns and crown ethers and lay the foundation for studies of the functional analogy between these two classes of molecular recognition agents.

Experimental Section

Materials. Salicylhydroxamic acid [H_3shi], 3-hydroxy-2-naphthoic acid, manganese(II) chloride, manganese(II) iodide, trichloroacetic acid,

(25) Lehn, J.-M. *Angew. Chem., Int. Ed. Engl.* **1988**, *27*, 89.
(26) Gokel, G. W.; Dishong, R. A.; Schultz, R. A.; Gatto, V. A. *Synthesis* **1982**, 997.
(27) (a) Lah, M. S.; Pecoraro, V. L. *Comments Inorg. Chem.* **1990**, *11*, 59. (b) Pecoraro, V. L.; Stemmler, A. J.; Gibney, B. R.; Bodwin, J. J.; Wang, H.; Kampf, J. W.; Barwinski, A. *Prog. Inorg. Chem.*, accepted for publication.
(28) Pecoraro, V. L. *Inorg. Chim. Acta* **1989**, *155*, 171.
(29) Lah, M. S.; Kirk, M. L.; Hatfield, W.; Pecoraro, V. L. *J. Chem. Soc., Chem. Commun.* **1989**, 1606.
(30) Gibney, B. R.; Stemmler, A. J.; Pilotek, S.; Kampf, J. W.; Pecoraro, V. L. *Inorg. Chem.* **1993**, *32*, 6008.
(31) Lah, M. S.; Pecoraro, V. L. *J. Am. Chem. Soc.* **1989**, *111*, 7258.
(32) Lah, M. S.; Pecoraro, V. L. *Inorg. Chem.* **1991**, *30*, 878.
(33) Kurzak, B.; Farkas, E.; Glowiak, T.; Kozlowski, H. *J. Chem. Soc., Dalton Trans.* **1991**, 163.
(34) Gibney, B. R.; Kampf, J. W.; Kessissiglou, D. P.; Pecoraro, V. L. *Inorg. Chem.* **1994**, *33*, 4840.
(35) Stemmler, A. J.; Kampf, J. W.; Pecoraro, V. L. *Inorg. Chem.* **1995**, *34*, 2271.
(36) (a) Stemmler, A. J.; Kampf, J. W.; Kirk, M. L.; Pecoraro, V. L. *J. Am. Chem. Soc.* **1995**, *117*, 6368−6369. (b) Stemmler, A. J.; Kampf, J. W.; Pecoraro, V. L. *Inorg. Chem.* **1995**, *34*, 2271−2272. (c) Stemmler, A. J.; Gibney, B. R.; Schneider, M.; Kampf, J. W.; Kirk, M. L.; Pecoraro, V. L. Manuscript in preparation.
(37) Kessissiglou, D. P.; Kampf, J. W.; Pecoraro, V. L. *Polyhedron* **1994**, *13*, 1379−1391. Stemmler, A. J.; Kampf, J. W.; Pecoraro, V. L. *Angew. Chem., Intl. Ed. Engl.*, in press.
(38) Lah, M. S.; Gibney, B. R.; Tierney, D. L.; Penner-Hahn, J. E.; Pecoraro, V. L. *J. Am. Chem. Soc.* **1993**, *115*, 5857−5858.
(39) Blake, A. J.; Gould, R. O.; Grant, C. M.; Milne, P. E. Y.; Reed, D.; Winpenny, R. E. P. *Angew. Chem., Int. Ed. Engl.* **1994**, *33*, 195.
(40) Blake, A. J.; Gould, R. O.; Milne, P. E. Y.; Winpenny, R. E. P. *J. Chem. Soc., Chem. Commun.* **1991**, 1453.
(41) Gutsche, C. D. *Acc. Chem. Res.* **1983**, *16*, 161−170.
(42) Gutsche, C. D. *Calixarenes: A Versitile Class of Macrocyclic Compounds*; Kluwer Academic Publishers: Boston, 1991; Vol. 3.
(43) Rauter, H.; Hillgeris, E. C.; Erxleben, A.; Lippert, B. *J. Am. Chem. Soc.* **1994**, *116*, 616−624.
(44) Fujita, M.; Yazaki, J.; Ogura, K. *J. Am. Chem. Soc.* **1990**, *112*, 5645.
(45) (a) Stang, P. J.; Chen, K. *J. Am. Chem. Soc.* **1995**, *117*, 1667−1668. (b) Stang, P. J.; Cao, D. H. *J. Am. Chem. Soc.* **1994**, *116*, 4981−4982. (c) Stang, P. J.; Zhdankin, V. V. *J. Am. Chem. Soc.* **1993**, *115*, 9808−9809.
(46) Anti-crowns are another class of inorganic molecular recognition agents that substitute metal ions into the oxygen positions of the crown ethers: Yang, X.; Knobler, C. B.; Zheng, Z.; Hawthorne, M. F. *J. Am. Chem. Soc.* **1994**, *116*, 7142.
(47) Gibney, B. R.; Wang, H.; Pecoraro, V. L. Manuscript in preparation.

trifluoroacetic acid, sodium hydroxide, lithium hydroxide, and potassium hydroxide were obtained from Aldrich Chemical Co. Manganese(II) bromide was purchased from Fluka. NMR solvents (CD_3OD, CD_3CN, and DMF-d_7) were purchased from Cambridge Isotopes. All other chemicals and solvents were reagent grade.

Abbreviations used: H_3shi, salicylhydroxamic acid; H_3dshi, 5-deuteriosalicylhydroxamic acid; H_3d_2shi, 3,5-dideuteriosalicylhydroxamic acid; H_3nha, 3-hydroxy-2-naphthylhydroxamic acid.

Metallacrown Nomenclature. The nomenclature for metallacrowns is as follows: $M'_mA_a[X\text{-}MC_{M^{n+}H(Z)}\text{-}Y]$, where *X* and *Y* indicate ring size and number of oxygen donor atoms, MC specifies a metallacrown, M and *n*+ are the ring metal and its oxidation state, H is the identity of the remaining heteroatom bridge, and (Z) is an abbreviation for the organic ligand containing the NO functionality. There are *m*′ captured metals (M′) and *a* bridging anions (A) bound to the ring oxygens and metals, respectively. A metal-encapsulated metallacrown is represented by $Mn(II)(OAc)_2[12\text{-}MC_{Mn(III)N(shi)}\text{-}4]$. This molecule has the core structure of 12-crown-4 with the carbon atoms replaced by Mn(III) and N atoms throughout the ring. The trianion of salicylhydroxamic acid (shi^{3-}) confers stability to the ring.[48,49] A single Mn(II) is captured by the hydroxamate oxygens, and there are two bridging acetates linking two ring metals to the captured metal. While not discussed here, a full treatment of additional descriptors of chirality for the ring and captured metal ions is given in ref 27b.

Preparation of Complexes. 1. Ligands. The ligands, 3-deuteriosalicylhydroxamic acid, 3,5-dideuteriosalicylhydroxamic acid, and 3-hydroxy-2-naphthylhydroxamic acid, were prepared as previously described.[30,34]

2. Metallacrown Complexes: General Procedure. A 50 mL solution of DMF containing a manganese(II) halide ($A = Cl^-$, Br^-, I^-) (5.0 mmol) was added to a 50 mL solution of DMF containing H_3shi (5 mmol) and the appropriate alkali metal ($M' = Li^+$, Na^+, K^+) trichloroacetate or trifluoroacetate salt (10 mmol). The resulting solution was allowed to stir for between 2 and 24 h and turned an olive green color, indicative of air oxidation of the Mn(II) to Mn(III). After gravity filtration, vapor diffusion with diethyl ether afforded the pure metallacrown complex, $(M'_mA_a)[12\text{-}MC_{Mn(III)N(shi)}\text{-}4]$ ($[(M'_mA_a)\cdot\mathbf{1}]$), in the yields indicated. The naphthohydroxamic acid-based metallacrowns, $[(M'_mA_a)\cdot\mathbf{2}]$, and the ring-deuterated salicylhydroxamic acid-based metallacrowns were synthesized in an analogous manner.

3. Salicylhydroxamic Acid-Based Metallacrowns. (a) Li^+-{$(LiCl_2)[12\text{-}MC_{Mn(III)N(shi)}\text{-}4]$} ($[(LiCl_2)\cdot\mathbf{1}]^-$). 67% yield (0.89 g). Anal. Calcd for $Li_2Cl_2Mn_4C_{49}H_{65}N_{11}O_{19}$: Mn, 15.5; Li, 1.0; C, 41.5; H, 4.6; N, 10.9. Found: Mn, 16.1; Li, 0.8; C, 41.7; H, 4.6; N, 10.6. FAB-MS(−) intact ion (M^-) 896.6 (51.7% of base).

(b) Li^+{$(LiBr_2)[12\text{-}MC_{Mn(III)N(shi)}\text{-}4]$} ($[(LiBr_2)\cdot\mathbf{1}]^-$). 66% yield (0.63 g). Anal. Calcd for $Li_2Br_2Mn_4C_{49}H_{67}N_{11}O_{20}$: Mn, 14.4; Li, 0.9; C, 38.6; H, 4.4; N, 10.1. Found: Mn, 14.3; Li, 0.9; C, 38.9; H, 4.3; N, 10.3. FAB-MS intact ion (M^-) 986.5 (10.9% of base).

(c) {$(Li(trifluoroacetate))[12\text{-}MC_{Mn(III)N(shi)}\text{-}4]$} ($[(LiTFA)\cdot\mathbf{1}]$). $MnF_2\cdot 4H_2O$ was used in an attempt to synthesize $[(LiF_2)\cdot\mathbf{1}]^-$; however, the reaction provided the trifluoroacetate complex. 27% yield (0.49 g). Anal. Calcd for $Li_1F_3Mn_4C_{51}H_{67}N_{11}O_{22}$: Mn, 14.9; Li, 0.5; C, 41.7; H, 4.6; N, 10.5. Found: Mn, 15.5; Li, 0.5; C, 42.0; H, 4.7; N, 10.5. FAB-MS intact ion (M^-) 827 (4.4% of base).

(d) {$(Li)[12\text{-}MC_{Mn(III)N(shi)}\text{-}4]$}$(I_3)^-$ ($[(Li)\cdot\mathbf{1}]^+$). Manganese(II) iodide was used in the synthesis, but air oxidation provided the triiodide salt of the metallacrown. 47% yield (1.1 g). Anal. Calcd for $Li_1I_3Mn_4C_{55}H_{81}N_{13}O_{22}$: Mn, 11.7; Li, 0.4; C, 35.0; H, 4.3; N, 9.7. Found: Mn, 12.2; Li, 0.4; C, 35.0; H, 4.2; N, 9.4. FAB-MS molecular ion (M^+) 827 (5.8% of base).

(e) $(NaCl)_2[12\text{-}MC_{Mn(III)N(shi)}\text{-}4]$ ($[(NaCl)_2\cdot\mathbf{1}]$) was synthesized as previously reported.[32]

(f) $(NaBr)_2[12\text{-}MC_{Mn(III)N(shi)}\text{-}4]$ ($[(NaBr)_2\cdot\mathbf{1}]$). 69% yield (1.3 g). Anal. Calcd for $Na_2Br_2Mn_4C_{43}H_{53}N_9O_{18}$: Mn, 15.6; Na, 3.3; C, 36.7; H, 3.8; N, 8.9. Found: Mn, 14.6; Na, 3.0; C, 36.4; H, 4.2; N, 8.9.

(g) $(KBr)_2[12\text{-}MC_{Mn(III)N(shi)}\text{-}4]$ ($[(KBr)_2\cdot\mathbf{1}]$). 86% yield (2.0 g). Anal. Calcd for $K_2Br_2Mn_4C_{49}H_{56}N_{11}O_{19}$: Mn, 14.0; K, 5.0; C, 37.5; H, 4.2; N, 9.8. Found: Mn, 13.7; K, 4.8; C, 37.6; H, 4.4; N, 9.8.

(h) $Mn(OAc)_2[12\text{-}MC_{Mn(III)N(shi)}\text{-}4]$ ($[Mn(OAc)_2\cdot\mathbf{1}]$) was synthesized as previously reported.[29]

4. Naphthohydroxamic Acid-Based Metallacrowns. (a) $Li(LiCl_2)[12\text{-}MC_{Mn(III)N(nha)}\text{-}4]$ ($[(LiCl_2)\cdot 2]^-$). 81% yield (1.6 g). Anal. Calcd for $Li_2Cl_2Mn_4C_{62}H_{70}N_{10}O_{20}$: Mn, 13.9; Li, 0.9; C, 47.2; H, 4.2; N, 8.9. Found: Mn, 14.2; Li, 1.2; C, 47.2; H, 4.4; N, 9.0. FAB-MS(−) molecular ion 1097 *m*/*z* (2.1% of base).

(b) $(NaCl)_2[12\text{-}MC_{Mn(III)N(nha)}\text{-}4]$ ($[(NaCl)_2\cdot 2]$). 74% yield (1.5 g). Anal. Calcd for $Na_2Cl_2Mn_4C_{62}H_{66}N_{10}O_{18}$: Mn, 13.9; Na, 2.9; C, 47.2; H, 4.2; N, 8.9. Found: Mn, 14.1; Na, 3.0; C, 46.9; H, 4.2; N, 8.6.

(c) $Mn(OAc)_2[12\text{-}MC_{Mn(III)N(nha)}\text{-}4]$ ($[Mn(OAc)_2\cdot 2]$). 61% yield (0.92 g). Anal. Calcd for $Mn_5C_{60}H_{61}N_8O_{22}$: Mn, 18.0; C, 47.4; H, 4.0; N,7.4. Found: Mn, 17.3; C, 47.4; H, 3.9; N, 7.3.

Methods. ^{1}H NMR spectra of the complexes were obtained on a Bruker 200 MHz FT-NMR spectrometer operating in the quadrature detection mode (^{1}H frequency, 200.1 MHz). Between 2000 and 5000 transients were accumulated over a 75 kHz bandwidth for each sample. The spectra contained 8000 data points, and the signal to noise ratio was improved by apodization of the free induction decay, which introduced a negligible 20 Hz line broadening. Baseline corrections of the NMR spectra were accomplished by a spline fit of baseline points chosen to minimize alteration of the peak line shape, position, and resolution. Chemical shifts were referenced to resonances due to residual protons present in the deuterated solvents. UV−visible spectra were recorded on a Perkin-Elmer Lambda 9 UV/vis/near-IR spectrophotometer equipped with a Perkin-Elmer 3600 data station. Positive and negative FAB mass spectra were acquired by the University of Michigan Mass Spectroscopy Facility. Electrospray ionization mass spectra (ESI-MS) were collected at the University of Michigan Protein and Carbohydrate Structure Facility. Elemental analyses were performed by the Analytical Services Laboratory in the Department of Chemistry at the University of Michigan. Variable-temperature magnetic susceptibility data were collected with a Quantum Concepts SQUID magnetometer. Molecular modeling was performed using Biosym Technologies InsightII on a Silicon Graphics Indigo^2 workstation.

X-ray Analysis. Suitable crystals of $(Li)[(LiCl_2)\cdot\mathbf{1}]$, $[(LiTFA)\cdot\mathbf{1}]$, $[(Li)\cdot\mathbf{1}](I_3)$, $[(NaBr)_2\cdot\mathbf{1}]$, and $[(KBr)_2\cdot\mathbf{1}]$ were obtained as described earlier. These crystals were mounted in glass capillaries, and diffraction data were collected on a Syntex $P2_1m/v$ or Siemens R3m/v diffractometer equipped with an LT-2 low-temperature device. Principal experimental parameters are given in Table 1. The data were reduced, the structures were solved via direct methods, and the model was refined by full-matrix least squares using either the SHELXTL PLUS[50a] program package (for $(Li)[(LiCl_2)\cdot\mathbf{1}]$, $[(NaBr)_2\cdot\mathbf{1}]$, and $[(KBr)_2\cdot\mathbf{1}]$) or the SHELEX-93[50b] program package (for $[(LiTFA)\cdot\mathbf{1}]$ and $[(Li)\cdot\mathbf{1}](I_3)$) on a VAXStation 3500. Hydrogen atoms were placed by using a riding model ($d_{C-H} = 0.96$ Å) and allowed to refine to a common isotropic *U*(H). Positional and thermal parameters for $(Li)[(LiCl_2)\cdot\mathbf{1}]$, $[(LiTFA)\cdot\mathbf{1}]$, $[(Li)\cdot\mathbf{1}](I_3)$, $[(NaBr)_2\cdot\mathbf{1}]$, and $[(KBr)_2\cdot\mathbf{1}]$ are given in the supporting information. Selected interatomic distances for $(Li)[(LiCl_2)\cdot\mathbf{1}]$, $[(LiTFA)\cdot\mathbf{1}]$, $[(Li)\cdot\mathbf{1}](I_3)$, $[(NaCl)_2\cdot\mathbf{1}]$, $[(NaBr)_2\cdot\mathbf{1}]$, $[(KBr)_2\cdot\mathbf{1}]$, and $[Mn(OAc)_2\cdot\mathbf{1}]$ are presented in Table 2. The ranges of selected interatomic bond angles for $(Li)[(LiCl_2)\cdot\mathbf{1}]$, $[(LiTFA)\cdot\mathbf{1}]$, $[(Li)\cdot\mathbf{1}](I_3)$, $[(NaCl)_2\cdot\mathbf{1}]$, $[(NaBr)_2\cdot\mathbf{1}]$, $[(KBr)_2\cdot\mathbf{1}]$, and $[Mn(OAc)_2\cdot\mathbf{1}]$ are presented in Table 3.

Results

Generic Description of $[12\text{-}MC_{Mn(III)N}\text{-}4]$ Structures. We will provide a general description of the basic 12-metallacrown-4 structure of $[(LiCl_2)\cdot\mathbf{1}]^-$, $[(LiTFA)\cdot\mathbf{1}]$, $[(Li)\cdot\mathbf{1}]^+$, $[(NaCl)_2\cdot\mathbf{1}]$, $[(NaBr)_2\cdot\mathbf{1}]$, $[(KBr)_2\cdot\mathbf{1}]$, and $[Mn(OAc)_2\cdot\mathbf{1}]$ using the $[(LiCl_2)\cdot\mathbf{1}]^-$ salt, illustrated in Figure 2, before delving into the subtleties of each compound. The solid state structures of $[Mn(OAc)_2\cdot\mathbf{1}]$[31] and $[(NaCl)_2\cdot\mathbf{1}]$[32] have been previously reported. Average

(48) For a description of hydroxamic acid ionization states, see Bagno, A.; Couzzi, C.; Scorrano, G. *J. Am. Chem. Soc.* **1994**, *116*, 916−924.
(49) For a description of hydroxamic acid ionization states, see Ventura, O. N.; Rama, J. B.; Turi, L.; Danenberg, J. J. *J. Am. Chem. Soc.* **1993**, *115*, 5754.
(50) (a) Siemens Analytical Servces, Madison, WI. (b) Sheldrick, G. M. *J. Appl. Crystallogr.*, in press.

Table 1. Crystallographic Data and Details of Refinement of (Li)[($LiCl_2$)·**1**], [(LiTFA)·**1**], [(Li)·**1**](I_3), [($NaBr)_2$·**1**], and [($KBr)_2$·**1**]

	compound				
	(Li)[($LiCl_2$)·**1**]	[(LiTFA)·**1**]	[(Li)·**1**](I_3)	[($NaBr)_2$·**1**]	[($KBr)_2$·**1**]
formula	$C_{50.5}H_{68.5}N_{11.5}O_6Mn_4Li_2Cl_2$	$C_{51}H_{67}N_{11}O_{22}Mn_4Li_1F_3$	$C_{52}H_{76}N_{12}O_{21}Mn_4Li_1I_3$	$C_{52}H_{72}N_{12}O_{20}Mn_4Na_2Br_2$	$C_{52}H_{72}N_{12}O_{20}Mn_4K_2Br_2$
mol wt, amu	1397.2	1469.84	1812.80	1610.92	1643.12
cryst syst	triclinic	monoclinic	monoclinic	monoclinic	monoclinic
space group	$P\bar{1}$ (No. 2)	*Cc* (No. 9)	$P2_1/n$ (No. 14)	$P2_1/n$ (No. 14)	$P2_1/n$ (No. 14)
a, Å	12.516(2)	20.261(6)	14.814(4)	14.131(4)	11.654(3)
b, Å	13.780(2)	19.577(5)	14.909(3)	13.845(3)	17.392(5)
c, Å	19.944(3)	16.134(5)	32.26(1)	16.539(4)	16.786(5)
α, deg	85.20(1)	90.000	90.000	90.000	90.000
β, deg	84.57(1)	99.81(2)	102.42(2)	96.17(2)	98.40(2)
γ, deg	72.18(1)	90.000	90.000	90.000	90.000
volume, Å^3	3254.3(9)	6306(3)	6959(3)	3217(1)	3366(2)
Z	2	4	4	2	2
temp, K	128	178	128	128	300
wavelength	Mo Kα (0.71073 Å)	Mo Kα (0.71073 Å)	Mo Kα (0.71073 Å)	Mo Kα (0.71073 Å)	Mo Kα (0.71073 Å)
quantity minimized	$\sum w(\|F_o\| - \|F_c\|)^2$	$\sum w(\|F_o^2 - F_c^2\|)^2$	$\sum w(\|F_o^2 - F_c^2\|)^2$	$\sum w(\|F_o\| - \|F_c\|)^2$	$\sum w(\|F_o\| - \|F_c\|)^2$
R	0.0773[a]	0.0871[c]	0.0684[c,d]	0.0416[a]	0.0649[a]
R_w	0.0887[b]	N/A	N/A	0.0419[b]	0.0850[b]

[a] $R = \sum||F_o - F_c||/|F_o|$. [b] $R_w = [\sum w(|F_o| - |F_c|)^2/\sum w|F_o|^2]^{1/2}$. [c] $wR^2 = [\sum w(F_o^2 - F_c^2)/\sum w(F_o^2)^2]^{1/2}$. [d] For comparison with structures refined on F_o, the conventional residual for $F_o \geq 4\sigma F_o$ is 0.0334.

Table 2. Selected Averaged Interatomic Distances (Angstroms) for the Salt Complexes of [12-$MC_{Mn(III)N(shi)}$-4] (**1**)

	(Li)[($LiCl_2$)·**1**]	[(LiTFA)·**1**]	[(Li)·**1**](I_3)	[($NaCl)_2$·**1**]	[($NaBr)_2$·**1**]	[($KBr)_2$·**1**]	[$Mn(OAc)_2$·**1**]
M(core)−O(oxime)	1.95(2)	1.967(3)	1.975(6)	2.44(2)	2.499(3)	2.828(5)	2.21(2)
M(core)−Mn	3.34(2)	3.343(3)	3.346(3)	3.42(2)	3.595(2)	3.897(2)	3.535(8)
M(core)−anion		1.94(2)		3.00(1)	2.985(2)	3.403(2)	
M(core)−O(DMF)	1.89(3)		1.976(6)	2.41(3)	2.371(3)	2.790(8)	
Mn−Mn	4.63(2)	4.62(10)	4.611(3)	4.59(1)	4.612(3)	4.607(5)	4.64(2)
Mn−halide	2.409(3)			2.43(1)	2.7701(8)	2.717(1)	
Mn−O (oxime)	1.884(8)	1.893(10)	1.880(2)	1.88(2)	1.882(3)	1.875(4)	1.88(2)
Mn−O (carbonyl)	1.956(8)	1.961(10)	1.966(2)	1.94(2)	1.964(3)	1.975(4)	1.96(2)
Mn−N (imine)	1.987(1)	1.951(12)	1.974(3)	1.98(1)	1.976(3)	1.973(5)	1.96(1)
Mn−O (phenolate)	1.860(7)	1.848(10)	1.864(2)	1.85(2)	1.874(3)	1.862(5)	1.84(2)
Mn−O (DMF)	2.276(8)	2.250(11)	2.289(2)	2.33(2)	2.289(3)	2.185(5)	2.25(1)
M(core)−M(core)				3.33(3)	3.28(1)	4.26(1)	
M(core)−O(plane)	0.63(1)	0.66(2)	0.64(1)	1.67(2)	1.64(1)	2.13(1)	1.20(1)

Table 3. Ranges of Selected Interatomic Bond Angles (Degrees) for the Salt Complexes of [12-$MC_{Mn(III)N(shi)}$-4] (**1**)

	(Li)[($LiCl_2$)·**1**]	[(LiTFA)·**1**]	[(Li)·**1**](I_3)	[($NaCl)_2$·**1**]	[($NaBr)_2$·**1**]	[($KBr)_2$·**1**]	[$Mn(OAc)_2$·**1**]
$O_H-M_n-O_C$	80.6(3)−81.4(3)	79.9(4)−81.8(5)	81.26(9)−81.57(9)	80.7(8)−81.4(8)	82.2(1)−81.7(1)	81.7(2)−81.8(2)	80(1)−82.1(9)
$O_H-M_n-N_I$	87.0(4)−89.0(4)	88.5(5)−90.0(5)	88.24(10)−88.88(10)	87.9(8)−88.8(2)	88.5(1)−88.0(1)	88.1(2)−89.5(2)	85(1)−90(1)
$N_I-M_n-O_P$	87.6(4)−89.9(4)	88.8(4)−89.8(5)	89.76(10)−90.22(10)	88.1(9)−100.2(8)	89.7(1)−89.0(1)	88.9(2)−89.3(2)	89(1)−90(1)
$O_P-M_n-O_C$	94.0(3)−102.1(3)	99.5(4)−101.7(4)	99.08(9)−100.07(9)	97.9(9)−100.2(8)	100.1(10)−100.4(1)	99.2(2)−99.9(2)	95(1)−103.6(9)
$M_n-O_H-M_C$	118.9(6)−121.8(4)	110.6(8)−123.4(9)	115.7(2)−124.2(2)	98.9(9)−104(1)	103.6(1)−122.9(1)	100.4(2)−120.6(2)	116(2)−126(1)
$O_H-M_C-O_H$	82.9(8)−85.7(9)	81.3(10)−86.0(9)	81.8(2)−86.0(2)	63.9(6)−65.1(7)	96.0(1)−98.8(1)	81.4(1)−82.2(1)	71.4(8)−75.4(8)

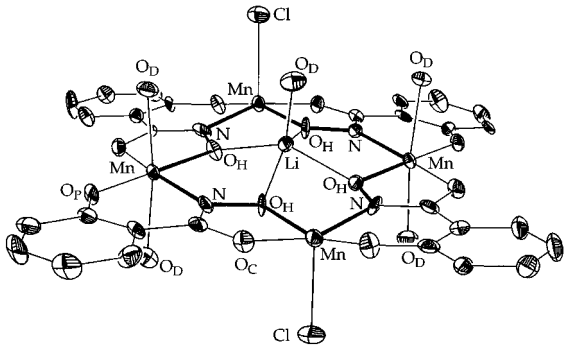

Figure 2. ORTEP diagram of ($LiCl_2$)[12-$MC_{Mn(III)N(shi)}$-4]$^-$ ([($LiCl_2$)·**1**]$^-$) with thermal ellipsoids at 50% probability. The 12-metallacrown-4 core, [Mn(III)NO]$_4$, is in bold; only the oxygens of the bound DMF molecules are shown and the hydrogen atoms are omitted for clarity.

chemically equivalent bond distances for all of the salt complexes of [12-$MC_{Mn(III)N(shi)}$-4] are given in Table 2, with the ranges of selected interatomic bond angles provided in Table 3. The cores of the novel lithium salt complexes [($LiCl_2$)·**1**]$^-$, [(LiTFA)·**1**], and [(Li)·**1**]$^+$ are illustrated in Figure 3; the cores of [($NaBr)_2$·**1**] and [($KBr)_2$·**1**] are shown in Figure 4.

The [12-$MC_{Mn(III)N(shi)}$-4] metallomacrocycle, illustrated in bold in Figure 2 for [($LiCl_2$)·**1**]$^-$, is very similar to the previously reported ($NaCl)_2$ and $Mn(OAc)_2$ salt complexes of this metallacrown.[31,32] Four-ring Mn(III) and four salicylhydroxamato (shi^{3-}) ligands construct the formally neutral [12-$MC_{Mn(III)N(shi)}$-4] core. The shi^{3-} is a binucleating tetradentate ligand that binds one ring metal (Mn) via the iminophenolate (N and O_P) in a 6-membered chelate and a second manganese (Mn) through the hydroxamate oxygens (O_C and O_H) in a juxtaposed 5-membered chelate. The resulting [Mn(III)$NO_H]_4$ ring system, shown in bold in Figures 2−4, orients four formally charged hydroxamate oxygens into the cavity (average cavity size 0.53 Å, average bite distance 2.64 Å) of a 12-membered macrocycle and is analogous to the $[CCO]_4$ core of 12-C-4 (cavity size 0.55 Å, bite distance 2.71 Å). The remainder of the coordination sites of the ring Mn(III) ions are filled by either DMF oxygens (O_D) or anions (Cl). The core metal (Li^+) is bound via the four cavity hydroxamate oxygens (O_H) and may bind additional solvents (O_D or O_w) or anions. The average adjacent ring Mn(III)−ring

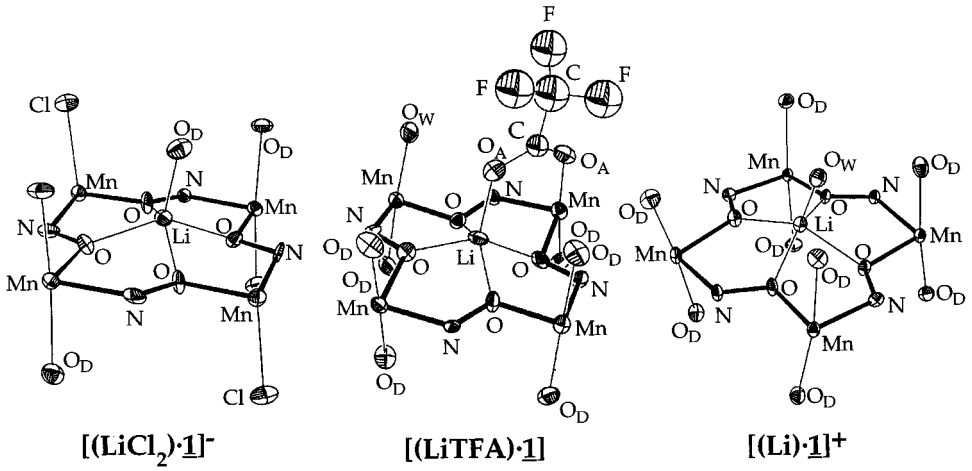

Figure 3. ORTEP diagrams of the metallacrown cores of $[(LiCl_2)\cdot\mathbf{1}]^-$, [(LiTFA)·**1**], and $[(Li)\cdot\mathbf{1}]^+$ with thermal ellipsoids at 50% probability. Lithium forms a 1:1 metal:metallacrown complex with either two chloride anions, one bridging trifluoroacetate ion or an unbound triiodide counteranion. The 12-metallacrown-4 core, $[Mn(III)NO]_4$, is in bold; only the oxygens of the bound DMF molecules are shown and the ligand peripheries are omitted for clarity.

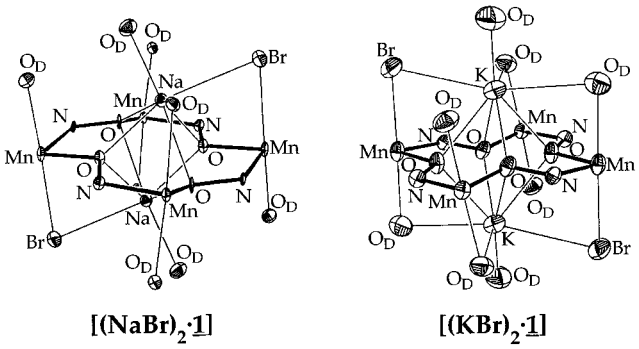

Figure 4. ORTEP diagrams of the metallacrown cores of $[(NaBr)_2\cdot\mathbf{1}]$ and $[(KBr)_2\cdot\mathbf{1}]$ with thermal ellipsoids at 50% probability. The larger alkali metal cations form 2:1 metal:metallacrown sandwich complexes.

Mn(III) separation is surprisingly invariant at 4.62(1) Å for all seven of the crystallographically characterized salt complexes of [12-$MC_{Mn(III)N(shi)}$-4] (**1**). The metallacrown macrocycles have dimensions[51] of 1.4 × 1.4 nm, demonstrating that they are true nanomolecular assemblies.

Description of the Structure of $(Li^+)\{(LiCl_2)$[12-$MC_{Mn(III)N(shi)}$-4]$\}$ ([$(LiCl_2)\cdot\mathbf{1}]^-$), $\{$(LiTFA)[12-$MC_{Mn(III)N(shi)}$-4]$\}$ ([(LiTFA)·1]), and $\{$(Li)[12-$MC_{Mn(III)N(shi)}$-4]$\}(I_3)$ ($[(Li)\cdot\mathbf{1}]^+$). The ORTEP diagram of $[(LiCl_2)\cdot\mathbf{1}]^-$ is provided in Figure 2, and the cores of $[(LiCl_2)\cdot\mathbf{1}]^-$, [(LiTFA)·**1**], and $[(Li)\cdot\mathbf{1}]^+$ are shown in Figure 3. Two of the ring Mn(III) ions in $[(LiCl_2)\cdot\mathbf{1}]^-$ are square pyramidal with Cl^- bound in the apical positions of this 5-coordinate geometry. The remaining ring Mn(III) ions in $[(LiCl_2)\cdot\mathbf{1}]^-$ are 6-coordinate with DMF oxygens bound in the axial positions of a Jahn−Teller elongated octahedron. In [(LiTFA)·**1**], the bound trifluoroacetate ion bridges between a ring Mn(III) ion and the core Li^+ ion, reminiscent of the acetate ions in $[Mn(OAc)_2\cdot\mathbf{1}]$ and of lariat ether metal complexes, with the remainder of the coordination sites of the pseudooctahedral ring Mn(III) ions filled with DMF or water oxygens. In $[(Li)\cdot\mathbf{1}]^+$, all of the ring Mn(III) ions are 6-coordinate with apical DMF solvents, and the triiodide counterion does not bind the metallacrown. This molecule is the first [12-$MC_{Mn(III)N(shi)}$-4] that does not have a bound anion, making this a useful starting material for anion-binding studies. These complexes are isolated as 1:1 metal:metallacrown complexes with Li^+ (Li^+ 5-coordinate ionic radius = 0.67 Å)[53] bound in the base of a square pyramid by the four hydroxamate oxygens of the metallacrown and apically via a single DMF oxygen in $[(LiCl_2)\cdot\mathbf{1}]^-$, a bridging trifluoroacetate ion in [(LiTFA)·**1**], or a single water oxygen in $[(Li)\cdot\mathbf{1}]^+$. In the structure of the analogous Li(12-C-4)Cl, the chloride ion is bound to the Li^+ ion at 2.290(4) Å as a contact ion pair.[52] The average Li^+-O_{crown} distances in $[(LiCl_2)\cdot\mathbf{1}]^-$, [(LiTFA)·**1**], and $[(Li)\cdot\mathbf{1}]^+$ are 1.96(1) Å, which are significantly shorter than the Li^+-O_{crown} bond distance of 2.128(2) Å in Li(12-C-4)Cl,[52] indicative of a stronger bonding interaction due to the partial negative charge on the metallacrown oxygens. The relative sizes of Li^+ (Li^+ 5-coordinate ionic radius = 0.67 Å)[53] and the metallacrown core, 0.51 Å, might suggest that the Li^+ would fit neatly within the cavity; however, the Li^+ resides 0.64 Å above the best least-squares plane of the metallacrown ring oxygen atoms. This suggests that the fifth ligand (O_{DMF}, O_{TFA}, or O_w) has a marked structural influence on cation binding. The complex $[(LiCl_2)\cdot\mathbf{1}]^-$, as isolated, is the Li^+ salt with the counterion unassociated with the metallacrown. Binding of a second Li^+ to the metallacrown might cause significant Li^+-Li^+ repulsion and is not observed in either the solid state or in solution.

Description of the Structures of $(NaBr)_2$[12-$MC_{Mn(III)N(shi)}$-4] ($[(NaBr)_2\cdot\mathbf{1}]$) and $(KBr)_2$[12-$MC_{Mn(III)N(shi)}$-4] ($[(KBr)_2\cdot\mathbf{1}]$). The cores of $[(NaBr)_2\cdot\mathbf{1}]$ and $[(KBr)_2\cdot\mathbf{1}]$ are illustrated in Figure 4. These metallacrowns form 1:2 host−guest complexes that are similar to the previously reported $[(NaCl)_2\cdot\mathbf{1}]$ salt complex of this metallacrown. Each sodium ion in $[(NaBr)_2\cdot\mathbf{1}]$ is 7-coordinate, composed of four metallacrown hydroxamate oxygens, one DMF oxygen bridging to a ring Mn(III), one singly bound DMF, and a single bromide ion bridging to a Mn(III). In contrast, the potassium ions in $[(KBr)_2\cdot\mathbf{1}]$ are 8-coordinate, composed of four metallacrown hydroxamate oxygens, two bridging DMF oxygens, one terminal DMF, and a bromide ion that bridges to the ring Mn(III). The cavity size of $[(NaBr)_2\cdot\mathbf{1}]$ is 0.58 Å, which is too small to accommodate the Na^+ ions (Na^+ 7-coordinate ionic radius = 1.12 Å)[53] that reside 1.64Å above and below the best least-squares plane of the metallacrown core oxygens. Similarly, the K^+ ions (K^+ 8-coordinate ionic radius = 1.51 Å)[53] reside 2.13 Å above and below the plane of the metallacrown core oxygens. The bromide ions are bridging between the ring Mn(III) ions and the encapsulated cations, as was seen for the chloride ions in the related

(51) Dimensions were measured by using macrocycle ring carbon atoms.

(52) Gingl, F.; Hiller, W.; Strähle, J.; Borgholte, H.; Dehnicke, K. *Z. Anorg. Allg. Chem.* **1991**, *606*, 91−96.
(53) Shannon, R. D. *Acta Crystallogr. Sec. A* **1976**, *32*, 751.

Table 4. Physical Characteristics and 1H NMR Resonance Assignments of for Salt Complexes of [12-$MC_{Mn(III)N(shi)}$-4]

		magnetic susceptibility			NMR[a]				
compound	UV−vis[a] λ_{max} (ϵ^b)	solid[c] (5 K)	solid[c] (300 K)	solution[a,c] (300 K)	H_3 resonance[d]	H_4 resonance[d]	H_5 resonance[d]	H_6 resonance[d]	acetate
(Li)[($LiCl_2$)·1]	361 (3923)	2.3	9.6	9.3	−15.8	−22.0	−18.9	+9.2	
(Li)[($LiBr_2$)·1]	361 (4107)	2.8	9.6	9.7	−16.0	−23.0	−18.7	+10.5	
[(Li)·1](I_3)	355 (4903)	2.4	9.8	9.6	−16.6	−23.8	−19.0	+13.1	
[$(NaCl)_2$·1]	361 (5066)	2.0	9.8	9.4	−17.2	−21.8	−19.6	+11.6	
[$(NaBr)_2$·1]	361 (3101)	2.3	9.8	9.6	−16.5	−22.4	−18.8	+9.5	
[$(KBr)_2$·1]	361 (3788)	2.6	9.6	9.3	−17.1	−23.3	−18.1	+12.2	
[$Mn(OAc)_2$·1]	361 (3827)	5.7	12.2	12.0	−15.9	−23.5	−17.2	+9.8	+56

[a] In DMF. [b] M^{-1} cm^{-1} per Mn(III). [c] μ_B per metallacrown. [d] ppm.

[$(NaCl)_2$·**1**] structure. While the sodium ions are displaced from the center of the metallacrown ring toward the bridging halide by 0.18 Å, the potassium ions in [$(KBr)_2$·**1**] reside above the center of the macrocycle. Because the Na^+ ions are shifted from the center of the cavity in [$(NaBr)_2$·**1**] and [$(NaCl)_2$·**1**], the sodium−oxime bond distances are inequivalent and the conformation of the metallacrown ring adopts a sofa configuration[54] similar to that observed in [Cu(II)12-$MC_{Cu(II)N(anha)}$-4]$^{2+}$.[34]

Magnetic Susceptibility Determinations. Variable-temperature magnetic susceptibility measurements on all of the alkali metal halide salt complexes of 12-$MC_{Mn(III)N(shi)}$-4 (**1**) were obtained from 2.5 to 350 K and the results are presented in Table 4. The solid state room-temperature value of the alkali metal salt complexes, ≈9.8 μ_B, is comparable to the 9.8 μ_B predicted for four independent $S = 2$ ions. Variable-temperature magnetic susceptibility measurements on all of the alkali metal halide salt complexes of **1** show weak intracluster antiferromagnetic coupling approaching a diamagnetic ground state at absolute zero. The presence of the core Mn(II) in [$Mn(OAc)_2$·**1**] elevates the room-temperature moment to 12.2 μ_B per metallacrown, and intracluster antiferromagnetic coupling results to an apparent $S = {}^5/_2$ ground state (μ_{eff} = 5.7 B. M.). The room-temperature solution susceptibilities, measured in DMF by using Evans' method,[55] are comparable to their solid state moments and are consistent with metallacrown integrity in DMF and weak intracluster exchange in the solid.

Solution Speciation of Metallacrowns. The solution structure of the salt complexes of [12-$MC_{Mn(III)N(shi)}$-4] (**1**) and [12-$MC_{Mn(III)N(nha)}$-4] (**2**) was addressed by using solution mass spectrometry. DMF solutions of the metallacrown complexes [($LiCl_2$)·**1**]$^-$, [($LiBr_2$)·**1**]$^-$, [(LiTFA)·**1**], and [(Li)·**1**]$^+$ in a 3-nitrobenzyl alcohol matrix gave strong molecular ions at *m*/*z* 827 (value calculated for $Li_1Mn_4C_{28}H_{16}N_4O_{12}$ is 827 g/mol) in the FAB-MS. The FAB-MS(−) of [($LiCl_2$)·**1**]$^-$ is presented in Figure 5 and is representative of the series. Peaks of higher mass to charge ratio due to the binding of halide ions were also observed, e.g., (LiCl)[12-$MC_{Mn(III)N(shi)}$-4] at *m*/*z* 861 and ($LiCl_2$)-[12-$MC_{Mn(III)N(shi)}$-4] at *m*/*z* 896, as shown in Figure 5. The observation of peaks at higher mass to charge ratio, consistent with anion binding, suggests that the anions remain bound to the metallacrown in solution. Additionally, the molecular ion of the naphthylhydroxamic acid-derived metallacrown, ($LiCl_2$)-[12-$MC_{Mn(III)N(nha)}$-4]$^-$, was observed at *m*/*z* 1027 (value calculated for $Li_1Mn_4C_{44}H_{24}N_4O_{12}$ is 1027 g/mol) with higher mass peaks consistent with chloride binding. The observed isotopic distributions are consistent with these assignments. The FAB-MS of the $(NaCl)_2$, $(NaBr)_2$, $(KBr)_2$, and $Mn(OAc)_2$ salt complexes of [12-$MC_{Mn(III)N(shi)}$-4] (**1**) did not show the expected molecular ions, probably due to the poor solubility and the poor volatility of the complexes.

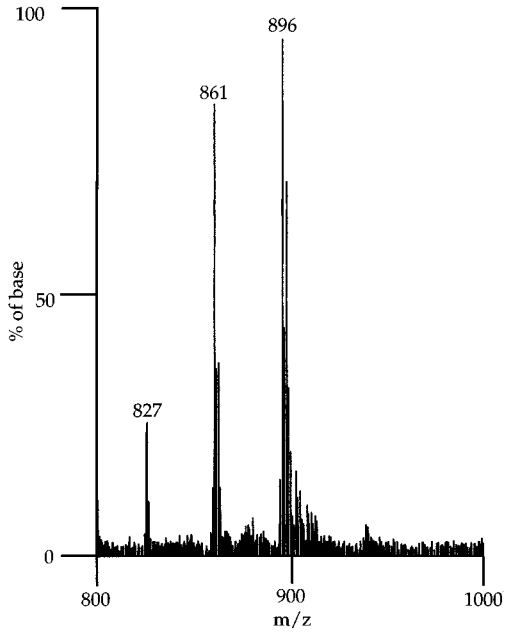

Figure 5. FAB-MS(−) of [($LiCl_2$)·**1**]$^-$ from DMF. The peak at *m*/*z* 827 (32% of base) is the molecular ion. The peaks at *m*/*z* 861 (82% of base) and 896 (base) correspond to the addition of one and two chloride ions to the molecular ion, respectively.

Electrospray ionization mass spectrometry (ESI-MS)[56−59] has been useful in confirming metallacrown solution integrity and was applied to all of the salt complexes of [12-$MC_{Mn(III)N(shi)}$-4].[34] The complexes [($LiCl_2$)·**1**]$^-$, [($LiBr_2$)·**1**]$^-$, [(LiTFA)·**1**], [(Li)·**1**]$^+$, and [($LiCl_2$)·**2**]$^-$ gave strong molecular ions at *m*/*z* 827 or 1027 in their ESI-MS(+), consistent with metallacrown solution integrity in acetonitrile and methanol and corroborating the FAB-MS results. In addition, the solution integrity of [$Mn(OAc)_2$·**1**] and [$Mn(OAc)_2$·**2**] was confirmed by observation of molecular ions consistent with the retention of metallacrown structure in solution from either CH_3CN or MeOH solution. The molecular ions of the neutral metallacrown salt complexes, [$Mn(OAc)_2$·**1**] and [$Mn(OAc)_2$·**2**], were observed at [M − 59]$^+$ due to loss of a single bridging acetate, suggesting that the anions might be labile in solution. The complexes [$(NaBr)_2$·**1**] and [$(KBr)_2$·**1**] did not yield satisfactory molecular ions via ESI-MS due to the neutral nature of these complexes.

(54) Scheidt, W. R.; Lee, Y. J. *Recent Advances in the Stereochemistry of Metallotetrapyrroles*; Springer-Verlag: Berlin, 1987; Vol. 64, p 2.
(55) (a) Evans, D. F. *J. Chem. Soc.* **1959**, 2003. (b) Bartle, K. D.; Dale, B. J.; Jones, D. W.; Maricic, J. *J. Magn. Reson.* **1973**, *12*, 286.
(56) (a) Smith, R. D.; Loo, J. A.; Edmonds, C. G.; Barinaga, C. J.; Udseth, H. R. *Anal. Chem.* **1990**, *62*, 882. (b)Kebarie, P.; Tang, L. *Anal. Chem.* **1993**, *65*, 972A.
(57) Katta, V.; Chowdhury, S. K.; Chait, B. T. *J. Am. Chem. Soc.* **1990**, *112*, 5348.
(58) Fenn, J. B.; Mann, M.; Meng, C. K.; Wong, S. F.; Whitehouse, C. M. *Science* **1989**, *246*, 64.
(59) (a) Colton, R.; Tedesco, V.; Traeger, J. C. *Inorg. Chem.* **1992**, *31*, 3865−3866. (b) Colton, R.; James, B. D.; Potter, I. D.; Traeger, J. C. *Inorg. Chem.* **1993**, *32*, 2626−2629.

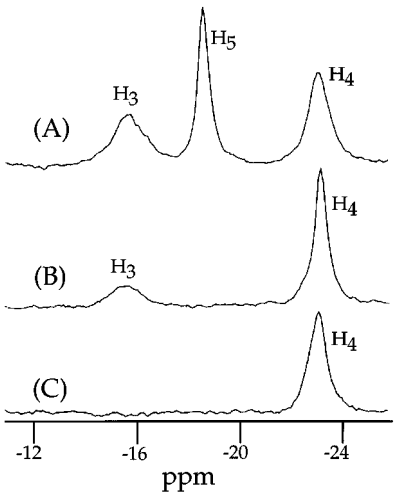

Figure 6. ^{1}H NMR spectra (−11 to −26 ppm) of (A) $(LiCl_2)$[12-$MC_{Mn(III)N(shi)}$-4]$^-$, (B) $(LiCl_2)$[12-$MC_{Mn(III)N(dshi)}$-4]$^-$, and (C) $(LiCl_2)$-[12-$MC_{Mn(III)N(d2shi)}$-4]$^-$ in DMF-d_7. The loss of one or two resonances upon singly or doubly deuterating the ligand periphery indicates that the three resonances shown are from a single species in solution. These spectra allow for the assignment of the resonances as shown.

Solution Integrity Studies via ^{1}H NMR. The solution integrity of the metallacrowns in DMF, acetonitrile, and methanol was investigated by using paramagnetically shifted ^{1}H NMR resonances from protons on the ligands. Each of the salt complexes of [12-$MC_{Mn(III)N(shi)}$-4] (**1**) displays three resonances in the range of −11 to −26 ppm with a fourth, usually obscured by the residual protons on the diamagnetic solvent, between +13.1 and +9 ppm. Figure 6 demonstrates that the observed resonances of $[(LiCl_2)\cdot\mathbf{1}]^-$ are due to a single species in solution, as selective deuteration of the ligand in the H_5 and then in both the H_3 and H_5 positions eliminates one and then two of the resonances. These spectra allow for the assignment of the resonances, as given in Table 4.[60] The ^{1}H NMR spectra of $[(LiCl_2)\cdot\mathbf{1}]^-$, $[(LiBr_2)\cdot\mathbf{1}]^-$, [(LiTFA)·**1**], and $[(Li)\cdot\mathbf{1}]^+$, illustrated in Figure 7, demonstrate that changes in the chemical shifts of the proton resonances can be attributed to anions bound to the paramagnetic metal center in the case of Cl^-, Br^-, and TFA^-. Binding of anions to the Mn(III) ions of the metallacrown ring causes a subsequent downfield shift in the H_4 resonance. These spectra further prove that the anions are bound in solution as the bromide and chloride spectra are not identical with the anion vacant complex, $[(Li)\cdot\mathbf{1}]^+$. Figure 8 illustrates the effect of cation binding on the chemical shifts of the resonances as the spectra of $[(LiBr_2)\cdot\mathbf{1}]^-$, $[(NaBr_2)\cdot\mathbf{1}]$, and $[(KBr_2)\cdot\mathbf{1}]$ are not identical. The resonances were assigned, as before, by using the selectively deuterated ligands, i.e. 3,5-dideuteriosalicylhydroxamic acid and 5-deuteriosalicylhydroxamic acid. While the mass spectrometry results do not allow for conclusions about the integrity of the $(NaCl)_2$, $(NaBr)_2$, and $(KBr)_2$ salt complexes of the metallacrown, their ^{1}H NMR spectra are consistent with the retention of gross metallacrown structure in solution. Analogous conclusions can be drawn from the ^{1}H NMR data of the naphthylhydroxamic acid-based metallacrowns.

(60) The assignment of the H_4 proton was determined by using the 4-methylsalicylhydroxamic acid-based [(LiCl)[12-$MC_{Mn(III)N(4-meshi)}$-4]. While the addition of the methyl to the phenyl ring causes perturbations of the ring electronics, and therefore the chemical shift of values of H_3, H_5, and H_6, the ^{1}H NMR spectrum showed loss of the H_4 signal with coincidental retention of the general line width and chemical shift of the other three signals. Gibney, B. R. Ph.D. Thesis, The University of Michigan, Ann Arbor, MI, 1994.

(61) (a) Evans, D. F. *J. Chem. Soc.* **1959**, 2003. (b) Bartle, K. D.; Dale, B. J.; Jones, D. W. Maricic, J. *J. Magn. Reson.* **1973**, *12*, 286.

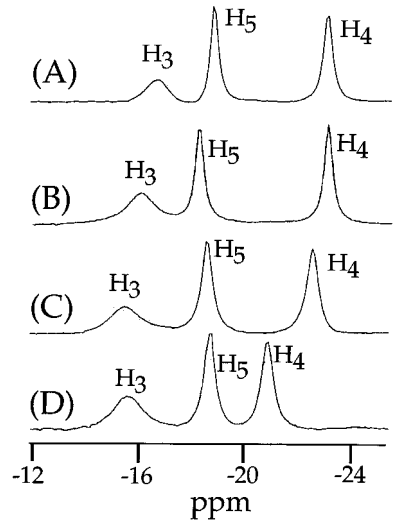

Figure 7. ^{1}H NMR spectra of (A) $[(Li)\cdot\mathbf{1}](I_3)$, (B) [(LiTFA)·**1**], (C) $(Li)[(LiBr_2)\cdot\mathbf{1}]$, and (D) $(Li)[(LiCl_2)\cdot\mathbf{1}]$ between −12 and −26 ppm. The binding of anions shifts the H_4 proton downfield. The resonances are assigned as shown by using selectively deuterated ligands. The H_6 proton resonances are downfield of TMS and show a similar line shape to the H_3 proton resonances.

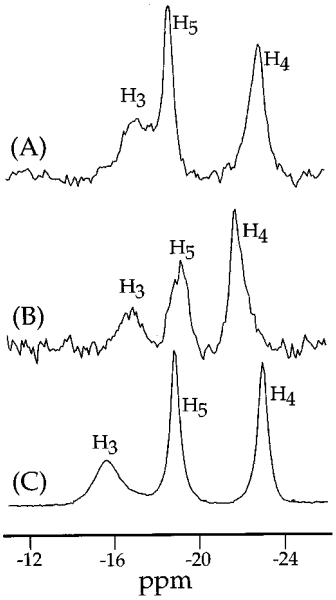

Figure 8. ^{1}H NMR spectra of (A) $[(KBr)_2\cdot\mathbf{1}]$, (B) $[(NaBr)_2\cdot\mathbf{1}]$, and (C) $[(LiBr_2)\cdot\mathbf{1}]^-$ between −11 and −26 ppm, demonstrating the cation effects on chemical shift. The resonances were assigned as shown by using the ligand deuterated analogues. The H_6 proton resonances are downfield of TMS and show similar line shapes to the H_3 proton resonances.

Structural Integrity Dependence on Concentration. The UV−visible spectra for all of the salt complexes of **1** vary linearly between 0.03 and 0.12 mM in methanol, acetonitrile, and DMF with the determined molar extinction coefficients given in Table 4. This adherence to Beer's law confirms that the metallacrown complexes do not dissociate at ≥0.04 mM concentrations.

Solution Dynamics Investigations via ^{1}H NMR. Kinetic information for ligand exchange in the [12-$MC_{Mn(III)N(shi)}$-4]−[12-$MC_{Mn(III)N(nha)}$-4] system was obtained in CH_3CN, DMF, and MeOH. While ligand exchange reactions between metallacrowns based on different ligands have thermodynamic penalties ($\Delta G \neq 0$), core metal/anion exchange reactions result in identical metallacrowns, thus simplifying interpretation of the data. Equimolar amounts of $(NaCl)_2$[12-$MC_{Mn(III)N(d2shi)}$-4] and $(NaCl)_2$-

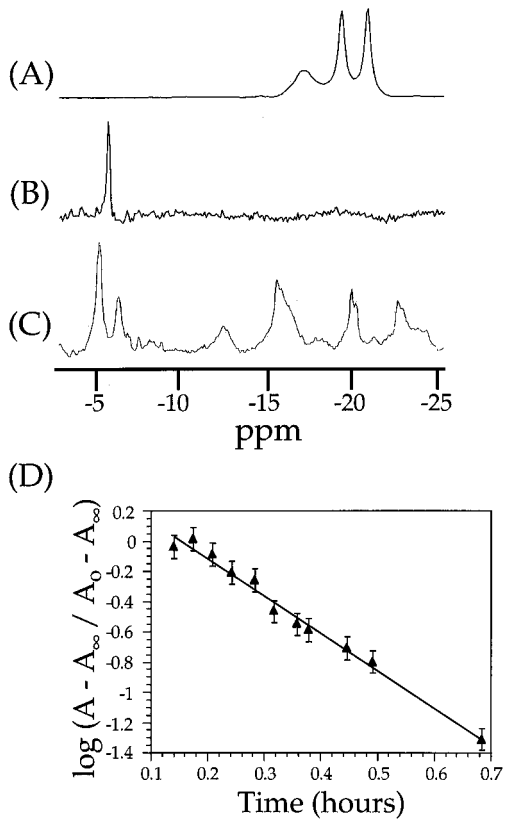

Figure 9. ^{1}H NMR spectra of (A) [$(NaCl)_2$·**1**], (B) [$(NaCl)_2$·**2**] from DMF-d_7, and (C) an equimolar mixture of [$(NaCl)_2$·**1**] and [$(NaCl)_2$·**2**] after 30 min in CD_3OD. (D) A plot of $\log[(A - A_\infty)/(A_o - A_\infty)]$ vs time (in hours) for a mixture of [$(NaCl)_2$·**1**] and [$(NaCl)_2$·**2**] in CD_3OD. The peak area, *A*, of the ^{1}H NMR resonance at −5.10 ppm was monitored.

[12-$MC_{Mn(III)N(nha)}$-4] were dissolved in CH_3CN or DMF and the ^{1}H NMR was observed as a function of time. Under these conditions, no ligand exchange was observed in CH_3CN or DMF within 1 week. Identical results are observed for all of the other salt complexes of [12-$MC_{Mn(III)N(shi)}$-4] (**1**) and [12-$MC_{Mn(III)N(nha)}$-4] (**2**) in CH_3CN and DMF. We conclude from these experiments that the salt complexes of [12-$MC_{Mn(III)N(shi)}$-4], (**1**) and [12-$MC_{Mn(III)N(nha)}$-4] (**2**) are intact in acetonitrile and DMF and do not undergo rapid ligand exchange reactions. The rates of cation/anion exchange reactions will be discussed in detail elsewhere.[47]

In methanol, however, ligand exchange was observed in the initial ^{1}H NMR recorded of the mixture of $(NaCl)_2$[12-$MC_{Mn(III)N(shi)}$-4] ([$(NaCl)_2$·**1**]) and $(NaCl)_2$[12-$MC_{Mn(III)N(nha)}$-4] ([$(NaCl)_2$·**2**]), as shown in Figure 9. A novel resonance at −5.10 ppm was followed as a function of time. The results of these experiments are shown as an inset of Figure 9, where $\log[(A - A_\infty)/(A_o - A_\infty)]$ vs time (in hours) is plotted for the monitored resonance (*A* is the normalized integrated area of the peak). The slope for the best fit line is 2.48 ± 0.02 h^{-1}. This treatment indicates that the approach to the equilibrium mixture is first-order, with an overall rate constant that is equal to the sum of the individual first-order rate constants from each participating species. This rapid exchange rate allowed for confirmation of the previously reported exchange rate of the vanadium metallacrown, 9-$MC_{(V(V)O)N(shi)}$-3, of 0.29 ± 0.02 h^{-1}.

Investigation of [$(LiCl_2)$·**1**]$^-$ and [$(LiCl_2)$·**2**]$^-$ displayed somewhat different behavior from that of their sodium counterparts. As was observed for the sodium salt complexes of **1** and **2**, equimolar mixtures of these two lithium metallacrowns yielded no observable ligand exchange in the ^{1}H NMR spectrum over the course of a week in DMF or CH_3CN. Additionally, this system was probed via FAB-MS, which corroborated the NMR results from acetonitrile and DMF. As a control, the $(LiCl_2)^-$ salt complexes of mixed-ligand metallacrowns (shi^{3-} and nha^{3-}), derived from synthesis, were observable in the FAB-MS. However, when dissolved in MeOH, no ligand exchange between [$(LiCl_2)$·**1**]$^-$ and [$(LiCl_2)$·**2**]$^-$ could be observed within 2 days by either ^{1}H NMR or mass spectrometry. The presence of a lithium ion, only 0.64 Å above the metallacrown core, greatly stabilizes the metallacrown in solution, thus reducing the rate of ligand exchange.

Discussion

Structural Comparison between 12-Metallacrown-4 and 12-Crown-4. The structural analogy between metallacrowns and crown ethers is best illustrated by direct comparison of the lithium chloride salt complexes of 12-C-4 and [12-MC-4] as enumerated in Table 5. The [12-$MC_{Mn(III)N(shi)}$-4] exhibits a neutral 12-membered heteroatom ring, containing four formally charged hydroxamate oxygens oriented into a central cavity of average size 0.53 Å. Similarly, the 12-C-4 possesses a 12-membered ring including four neutral ether oxygens in a cavity of size 0.55 Å.[52] Both the metallacrown and the crown ether are neutral moieties that bind Li^+ in a 1:1 metal:(metalla)-crown ratio. The 5-coordinate Li^+, ionic radius 0.67 Å,[53] resides above the cavity in the both the crown ether (0.93 Å displacement) and the metallacrown (0.64 Å displacement). The lithium ion is bound apically via a DMF oxygen in $(LiCl_2)$[12-$MC_{Mn(III)N(shi)}$-4]$^-$ ([$(LiCl_2)$·**1**]$^-$); however, in the organic crown ether complex, Li^+ forms a contact ion pair with chloride [2.290-(4) Å].[52] In the metallacrown, [$(LiCl_2)$·**1**]$^-$, the two chloride anions bind the Lewis acidic Mn(III) ring metals at 2.409(3) Å and make no bonding interactions with the encapsulated Li^+. In [(LiTFA)·**1**], the trifluoroacetate ion bridges between the ring Mn(III) ion and the core Li^+ ion, a binding mode not observed in simple crowns but synthetically engineered into lariat ethers.[18−20] In [(Li)·**1**]$^+$, the triiodide anion is not associated with either the core Li^+ or the ring Mn(III) ions of the metallacrown. The crown ether complex is a classical "crown" conformation with a crystallographically imposed C_4 axis along the Li−Cl bond, with the ethylene carbons below the plane of the oxygens away from the encapsulated cation.[52] In the 12-metallacrown-4's, the enhanced rigidity of the metallacrown ring obviates the possibility of the classic crown conformation, preferring instead a planar or slightly bowed conformation.

Comparison of the structures of larger alkali metal cation complexes with 12-C-4 and 12-metallacrown-4 is also instructive. The metallacrown prefers to bind Na^+ (Na^+ 7-coordinate ionic radius = 1.12 Å) and K^+ (K^+ 8-coordinate ionic radius = 1.51 Å) in a 2:1 metal:metallacrown stoichiometry, whereas 12-C-4 complexes with these larger alkali metal cations are of a 1:2 metal:crown stoichiometry.[62] The metallacrown retains a bite distance and cavity size similar to those of the organic crown ether, and the metal−oxygen distances between crowns and metallacrowns are comparable, as shown in Table 5.[62,63]

Physically these two classes of crown compounds are markedly divergent. While the UV−visible spectrum of [$(LiCl_2)$·**1**]$^-$ shows a λ_{max} at 361 nm (ϵ = 13 500 M^{-1} cm^{-1}

(62) Na(12-C-4)$_2$: (a) Mason, E.; Eick, H. *Acta Crystallogr.* **1982**, *B38*, 1821. (b) Ahle, A.; Neumuller, B.; Pebler, J.; Atanasov, M.; Dehnicke, K. *Z. Anorg. Allg. Chem.* **1992**, *615*, 131. K(12-C-4)$_2$: (c) Kamitori, S.; Hirotsu, K.; Higuchi, T. *J. Am. Chem. Soc.* **1987**, *109*, 2409.

(63) Na(15-C-5): (a) Schreiner, B.; Dehnicke, K.; Fenske, D. *Z. Anorg. Allg. Chem.* **1993**, *619*, 1127. K(18-C-6): (b) Luger, P.; André, C.; Rudert, R.; Zobel, D.; Knöchel, A.; Krause, A. *Acta Crystallogr.* **1992**, *B48*, 33.

Table 5. Structural Comparison of Crown Ether, Porphyrin, Phthalocyanine, and 12-Metallacrown-4 Complexes of Alkali Metals[a]

compound	bite distance (Å)	cavity size (Å)	metal:host	M−O distance (Å)	M−O_{plane} (Å)	ref
			Crown Ethers			
$[Li(12\text{-}C\text{-}4)]^+$	2.71	0.55	1:1	2.13	0.93	52
$[Na(12\text{-}C\text{-}4)_2]^+$	2.80	0.64	1:2	2.48	1.49	62a
$[K(12\text{-}C\text{-}4)_2]^+$	2.71	0.55	1:2	2.90	2.84	62b
$[Na(15\text{-}C\text{-}5)]^+$	2.72	0.76	1:1	2.67	1.12	63a
$[K(18\text{-}C\text{-}6)]^+$	2.82	1.44	1:1	2.84	0.18	63b
			Metallacrowns			
$(Li)[12\text{-}MC_{Mn(III)N(shi)}\text{-}4]^+$	2.65	0.5	1:1	1.95	0.63	
$(LiTFA)[12\text{-}MC_{Mn(III)N(shi)}\text{-}4]$	2.65	0.50	1:1	1.97	0.66	
$(LiCl_2)[12\text{-}MC_{Mn(III)N(shi)}\text{-}4]^-$	2.66	0.51	1:1	1.97	0.64	
$(NaCl)_2[12\text{-}MC_{Mn(III)N(shi)}\text{-}4]$	2.63	0.50	2:1	2.43	1.66	32
$(NaBr)_2[12\text{-}MC_{Mn(III)N(shi)}\text{-}4]$	2.65	0.58	2:1	2.49	1.64	
$(KBr)_2[12\text{-}MC_{Mn(III)N(shi)}\text{-}4]$	2.62	0.53	2:1	2.82	2.13	
$Mn(OAc)_2[12\text{-}MC_{Mn(III)N(shi)}\text{-}4]$	2.67	0.53	1:1	2.21	1.20	31
			Porphyrins			
$[Li(TMPP)]^-$	2.78	0.68	1:1	2.03(M−N)	0.0	64a
$[Na_2(OEP)]$	2.90	0.69	2:1	2.48(M−N)	1.39	64b
$[K_2(OEP)]$	2.92	0.70	2:1	2.77(M−N)	1.85	64b
			Phthalocyanines			
$[Li(pc^{\bullet})]$	2.75	0.58	1:1	1.94(M−N)	0.0	65
$[K_2(pc)]$	2.78	0.60	2:1	2.90(M−N)	2.13	66

[a] TMPP, *meso*-tetrakis(3,4,5-trimethoxyphenyl)porphyrin dianion; OEP, octaethylporphyrin dianion; $pc^{\bullet}$, phthalocyanine dianion p-cation radical; pc = phthalocyanine dianion.

per metallacrown), the visible spectrum of the crown ether is featureless. The organic crown is diamagnetic as a Li^+ complex, whereas the metallacrown is highly paramagnetic with a room-temperature magnetic moment of 9.3 μ_B.

Structural Comparison of Alkali Metal Complexes of Porphyrins, Phthalocyanine, and [12-MC-4]. The similarities in the structures of alkali metal complexes of porphyrins, alkali metal complexes of phthalocyanines, and alkali metal halide salt complexes of $[12\text{-}MC_{Mn(III)N(shi)}\text{-}4]$ (**1**) are remarkable, as enumerated in Table 5. The bite distance and cavity size of the porphyrin dianion (2.86 and 0.69 Å, respectively) and phthalocyanine dianion (2.76 and 0.59 Å) are slightly larger than those of 12-metallacrown-4 (2.65 and 0.53 Å) due to the larger number of atoms in the porphyrin and phthalocyanine macrorings. The dimensions of the metallacrown (1.4 × 1.4 nm) and phthalocyanine (1.2 × 1.2 nm) are comparable, with the porphyrin being slightly smaller (0.7 × 0.7 nm) due to the lack of phenyl rings.[51] All three structure types are amenable to alteration of their peripheries for the construction of larger nanomolecular assemblies. In fact, molecular modeling shows the dimensions of $[12\text{-}MC_{Mn(III)N(nha)}\text{-}4]$ (**2**) to be 1.8 × 1.8 nm.[51]

The porphyrin moiety, the phthalocyanine dianion π-cation radical, and the metallacrown **1** bind Li^+ in a 1:1 ligand:metal ratio, but the porphyrin[64] and phthalocyanine[65] contain rare square planar 4-coordinate Li^+ ions in the best least-squares plane of the macrocycle. The Li^+ encapsulated by the metallacrown is 5-coordinate in the solid state. NMR (^{7}Li NOESY) has demonstrated that the porphyrin dianion can also be prepared as the dilithium complex, but the crystal structure has not been reported.[64] It has been suggested that in this case the porphyrin is only bidentate to each of the Li^+ ions, which allows for minimization of cationic repulsion. This binding motif is not observed in the metallacrown, which can be isolated with a single bound Li^+ ion and a solvated Li^+ counterion.

Porphyrins have been structurally characterized as both the sodium and potassium complexes, both of which form 1:2 host−guest sandwich type complexes similar to that observed for the metallacrown (**1**).[64] The phthalocyanine dianion has been structurally characterized as the dipotassium complex.[66,67] The metal−ligand bond distances for the alkali metal complexes of porphyrins, phthalocyanines, and **1** are comparable. Due to the larger cavity of the porphyrin and phthalocyanine, the cation out of plane distances are shorter than those of the metallacrown, as enumerated in Table 5. While the porphyrin and phthalocyanine dianions are utilized for their respective alkali metal complexes, the metallacrown ring is formally neutral and binds alkali metals in similar stoichiometries with similar bond lengths. Additionally, the metallacrown is anion selective, a rare feature in molecular recognition chemistry.

This correlation between metallacrown, porphyrin, and phthalocyanine structures is extremely important when one considers the architectural utility of porphyrins and phthalocyanines. Porphyrin-based supramolecular assemblies are used in a plethora of applications, including α-helical peptide supports[68] and templates for electron transfer reactions.[69] Liquid crystals based on phthalocyanines have been prepared.[70] The proven variability of the metallacrown peripheral ligand architecture coupled with the topological similarity to porphyrin and phthalocyanine structures suggests that the metallacrown could serve as a supramolecular template.

In terms of reactivity, the alkali metal porphyrin complexes are potent synthons for the preparation of transition metal porphyrin complexes, especially those of the early transition

(64) (a) Arnold, J. *J. Chem. Soc., Chem. Commun.* **1990**, 976. (b) Arnold, J.; Dawson, D. Y.; Hoffman, C. G. *J. Am. Chem. Soc.* **1993**, *115*, 2707. (c) Brand, H.; Capriottti, J. A.; Arnold, J. *Inorg. Chem.* **1994**, *33*, 4334.

(65) Sugimoto, H.; Mori, M.; Masuda, H.; Taga, T. *J. Chem. Soc., Chem. Commun.* **1986**, 962.

(66) Ziolo, R. F.; Günther, W. H. H.; Troup, J. M. *J. Am. Chem. Soc.* **1981**, *103*, 4629.

(67) Ziolo, R. F.; Extine, M. *Inorg. Chem.* **1981**, *20*, 2709.

(68) (a) Sasaki, T.; Kaiser, E. *J. Am. Chem. Soc.* **1989**, *111*, 380. (b) Åkerfeldt, K. S.; Kim, R. M.; Camac, D.; Groves, J. T.; Lear, J. D.; DeGrado, W. F. *J. Am. Chem. Soc.* **1992**, *114*, 9656.

(69) (a) Sessler, J. L.; Wang, B.; Harriman, A. *J. Am. Chem. Soc.* **1995**, *117*, 704. (b) Král, V.; Sessler, J. L.; Furuta, H. *J. Am. Chem. Soc.* **1992**, *114*, 8704. (c) Furuta, H.; Magda, D.; Sessler, J. L. *J. Am. Chem. Soc.* **1991**, *113*, 978. (d) Harriman, A.; Magda, D. J.; Sessler, J. L. *J. Phys. Chem.* **1991**, *95*, 1530.

(70) (a) Piechocki, C.; Simon, J.; Skoulios, A.; Guillon, D.; Weber, P. *J. Am. Chem. Soc.* **1982**, *104*, 5245. (b) Cook, M. J.; Daniel, M. F.; Harrison, K. J.; McKeown, N. B.; Thomson, A. J. *J. Chem. Soc., Chem. Commun.* **1987**, 1086. (c) Piechocki, P.; Simon, J. *Nouv. J. Chem.* **1985**, *9*, 159.

metals, e.g., Sc(III),[71] Zr(IV),[72−74] and V(III).[75] Similarly, the alkali metal complexes of the phthalocyanine dianion have yielded late transition metal complexes. By analogy, these observations suggest that the structurally similar alkali metal halide salt complexes of the metallacrown [12-$MC_{Mn(III)N(shi)}$-4] may be capable of encapsulating a wide variety of transition metal ions via metathesis reactions. In fact, all of the characterized alkali metal halide salt complexes of **1** can be converted to $Mn(OAc)_2$[12-$MC_{Mn(III)N(shi)}$-4] upon the addition of a single equivalent of $Mn(OAc)_2$.[47] Conversely, the structural similarities between metallacrowns, porphyrins, and phthalocyanines suggest that one should consider the porphyrin and phthalocyanine dianions as selective cation recognition agents with transition metal specificity. In fact, Ziolo et al. hinted at the molecular recognition aspects of phthalocyanine when noting the increased K−N bond lengths of $[(K)_2(pc)(18\text{-}C\text{-}6)_2]$[66] compared to $[(K)_2(pc)(DMF)_4]$,[67] which was a clear indication of competitive potassium ion coordination between the organic crown and phthalocyanine.

Conclusions

12-Metallacrown-4, an inorganic molecular recognition agent of nanomolecular size, is a structural analogue of 12-crown-4 with the methylene carbons replaced by transition metals and nitrogen atoms and having a cavity size and bite distance similar to those of 12-crown-4. The metallacrown is simultaneously cation and anion selective, a rare feature in organic molecular recognition agents. A general one-step, high-yield synthesis provides gram quantities of a variety of alkali metal halide complexes of [12-$MC_{Mn(III)N(shi)}$-4] suitable for X-ray diffraction studies. The metrical parameters of the metallacrown are essentially invariant regardless of the number and type of cation(s)/anion(s) bound to the metallamacrocycle. While Li^+ binds the metallacrown in a 1:1 metal:metallacrown ratio, larger alkali metal cations bind in 1:2 host−guest stoichiometries. The structural parameters of the alkali metal halide salt complexes of [12-$MC_{Mn(III)N(shi)}$-4] are comparable to those of the alkali metal complexes of 12-crown-4, porphyrins, and phthalocyanines. One exception is that the $Li-O_{crown}$ bond distances in the metallacrown are considerably shorter than those in 12-C-4, which is indicative of a stronger bonding interaction. Furthermore, the metallacrown binds anions on the ring metal ions, which may bridge to the core metals, whereas the other macrocycles bind anions via the core metal.

Intact metallacrowns are the active molecular recognition agent in solution, as proven by using a variety of solution probes. Mass spectrometry coupled with ^{1}H NMR spectroscopy provides irrefutable evidence of metallacrown solution integrity for all of the salt complexes of [12-$MC_{Mn(III)N(shi)}$-4] (**1**) and [12-$MC_{Mn(III)N(shi)}$-4] (**2**). The mass spectra indicated that the cations remained bound to the metallacrowns with labile anions. ^{1}H NMR spectroscopy of the metallacrowns based on the selectively deuterated ligands, i.e., $dshi^{3-}$ and d_2shi^{3-}, allowed assignment of the ^{1}H NMR spectra of all of the complexes and proved that the resonances result from a single species in solution. The differences in the ^{1}H NMR of a series of anion derivatives of [(Li)12-$MC_{Mn(III)N(shi)}$-4] ($[(Li)\cdot\mathbf{1}]^+$), unambiguously showed that the anions remain bound to the metallacrown in solution and corroborated the FAB-MS results. ^{1}H NMR of the series $[(LiBr_2)\cdot\mathbf{1}]^-$, $[(NaBr)_2\cdot\mathbf{1}]$, and $[(KBr)_2\cdot\mathbf{1}]$ demonstrated that the core cations, in at least two of the three metallacrown salt complexes, remain bound to the metallacrown in solution.

These studies are integral to the structural analogy between metallacrowns and crown ethers, and they lay the structural basis for study of the functional analogy. The proven structural integrity of the metallacrowns supports the concept of using metallacrowns as cation/anion selective agents and as nanomolecular architectures for the construction of supramolecular systems. The variability of the ring metal, structural motif, ligand peripheral architecture, ligand donor set, and bound salt firmly establish the synthetic prowess of the metallacrown analogy for the rational design of nanomolecular inorganic molecular recognition agents.

Acknowledgment. We greatly appreciate the National Institutes of Health (Grant No. GM39406) and the A. P. Sloan Foundation for support of this work. B.R.G. and H.W. thank the University of Michigan for both Smeaton Graduate and Undergraduate Fellowships.

Supporting Information Available: Tables providing a complete crystallographic summary, anisotropic thermal parameters of all nonhydrogen atoms, fractional atomic positions all atoms, a complete set of bond distances, and a complete set of bond angles for $(Li)[(LiCl_2)\cdot\mathbf{1}]$, $[(LiTFA)\cdot\mathbf{1}]$, $[(Li)\cdot\mathbf{1}](I_3)$, $[(NaBr)_2\cdot\mathbf{1}]$, and $[(KBr)_2\cdot\mathbf{1}]$ (73 pages). Ordering information is given on any current masthead page.

IC960371+

(71) Arnold, J.; Hoffman, C. G. *J. Am. Chem. Soc.* **1990**, *112*, 8620.
(72) Arnold, J.; Johnson, S. E.; Knobler, C. B.; Hawthorne, M. F. *J. Am. Chem. Soc.* **1992**, *114*, 3996.
(73) Brand, H.; Arnold, J. *J. Am. Chem. Soc.* **1992**, *114*, 2266.
(74) Kim, H.-J.; Whang, D.; Kim, K.; Do, Y. *Inorg. Chem.* **1993**, *32*, 360.
(75) Berreau, L. M.; Hays, J. A.; Young, V. G. J.; Woo, L. K. *Inorg. Chem.* **1994**, *33*, 105.